

Collective excitations in realistic quantum wires

This article has been downloaded from IOPscience. Please scroll down to see the full text article.

1996 J. Phys.: Condens. Matter 8 L325

(<http://iopscience.iop.org/0953-8984/8/23/002>)

View [the table of contents for this issue](#), or go to the [journal homepage](#) for more

Download details:

IP Address: 171.66.16.206

The article was downloaded on 13/05/2010 at 18:24

Please note that [terms and conditions apply](#).

LETTER TO THE EDITOR

Collective excitations in realistic quantum wires

Arne Brataas[†] A G Mal'shukov[‡] Vidar Gudmundsson[§] and K A Chao[†]

[†] Department of Physics, Norwegian University of Science and Technology,
N-7034 Trondheim, Norway

[‡] Institute of Spectroscopy, Russian Academy of Sciences, 142092 Troitsk,
Moscow Region, Russia

[§] Science Institute, University of Iceland, Dunhaga 3, IS-107 Reykjavik, Iceland

Received 18 March 1996

Abstract. We have used the Hartree–Fock random phase approximation to study the interacting electron gas in a quantum wire. The spectra of intersubband spin-flip excitations reveal a considerable red shift with respect to single-particle Hartree–Fock energies. That signals the appearance of collective intersubband spin-density excitations due to the exchange interaction. The long-wavelength dispersions of the intrasubband collective spin-density excitations are linear but the sound velocities are renormalized due to the exchange interaction and screening. The in-phase intrasubband charge-density excitation has the long-wavelength form $q[-\ln(q)]^{1/2}$. We found good qualitative agreement of our results with experimental observations.

A semiconductor quantum wire can be fabricated by applying a voltage with a microstructured gate to a 2D electron gas. The single-particle energy (SPE) spectrum typically consists of subbands separated by several meV. At a 1D electron density of about 10^6 cm^{-1} more than one subband can be occupied. In recent years progress has been made in the spectroscopic study of such systems. In angular resolved Raman spectra of GaAs quantum wires [1–3] collective spin-density excitations (SDE) and charge-density excitations (CDE or plasmons) were observed. The measured spectra cover low to high frequencies and for low-frequency intrasubband excitations the wavevector dependence of the spin-wave energy was found to be linear. The correct interpretation of these experiments allows us not only to understand the interesting physical processes but also to access important physical parameters.

The exchange interaction is crucial to the collective intrasubband and intersubband SDE. Similar to the direct long-range Coulomb interaction which leads to the depolarization shift of single-particle excitations and to the appearance of collective plasma modes, exchange interaction gives rise to the red shift of SPE. If the red shift is sufficiently large, the collective SDE with a sizable oscillator strength splits off the continuum of SPE. For semiconductor quantum wells such split off appears in the Hartree–Fock random phase approximation (HF-RPA) [4–7]. Thus it is important to perform a HF-RPA analysis on collective electron excitations in a realistic GaAs quantum wire with full Coulomb interaction and to compare the results with measured spectra [2, 3]. The self-consistent and conserving [8] HF-RPA is suitable for this task because we will calculate the two-particle spectra but not single-particle properties. As in using any approximation, the HF-RPA calculation also contains error. However, our HF-RPA results agree very well with experimental measurements.

In this letter we will first outline the HF-RPA method of expressing the spin or charge correlation functions in terms of the corresponding spin- or charge-density-induced matrix, which satisfies an eigenvalue matrix equation. In a realistic quantum wire, for high-energy

intraband excitations and for excitation spectra when more than one subband is occupied, the self-consistent equations have to be solved numerically. However, for the case in which only one subband is occupied the analytical expressions of SDE and CDE are derived. With the additional approximation applied to the HF-RPA analytical solutions they reduce to known results. This may be coincidental but is outside the central theme of this letter.

In order to define the quantum wire, let us start from an electron gas in a narrow quantum well with interfaces parallel to the x - y plane and the well width smaller than any other relevant length scales. We consider the realistic experimental situation that only the lowest subband in the quantum well is occupied, so the motion of electrons in the z direction can be ignored. By applying a properly designed gate potential, a quantum wire along the x axis is fabricated with a longitudinal constant electrostatic potential, but a transverse parabolic one $V_c(y) = m^* \omega_0^2 y^2 / 2$ along the y axis, where m^* is the electronic effective mass. The quantum wire has a finite length L_x , and we assume periodic boundary conditions. In the absence of electron–electron interactions, the single-particle eigenfunctions are simply $\Psi_{nk}(x, y) = L_x^{-1/2} e^{ikx} \psi_{nk}(y)$ with the corresponding eigenenergies $E_{nk} = \hbar \omega_0 (n + 1/2) + (\hbar^2 k^2) / (2m^*)$, where n is the subband index, $k = \text{integer} \times 2\pi / L_x$ and $\psi_{nk}(y)$ is the harmonic oscillator wavefunction. The transverse confinement length of the electrons is $l_0 = [\hbar / (m^* \omega_0)]^{1/2}$.

When the electron–electron interaction is turned on we will use the HF approximation

$$\left\{ -\frac{\hbar^2}{2m^*} \nabla^2 + V_c(y) + \frac{2e^2}{\kappa} \int d\mathbf{r}' \sum_b f_b \frac{|\Psi_b(\mathbf{r}')|^2}{|\mathbf{r} - \mathbf{r}'|} \right\} \Psi_a(\mathbf{r}) - \frac{e^2}{\kappa} \int d\mathbf{r}' \sum_b f_b \frac{\Psi_b^*(\mathbf{r}') \Psi_b(\mathbf{r})}{|\mathbf{r} - \mathbf{r}'|} \Psi_a(\mathbf{r}') = \epsilon_a^{HF} \Psi_a(\mathbf{r}) \quad (1)$$

to derive a complete orthonormal basis $\{\Psi_a(\mathbf{r})\}$ of quasi-particle Hartree–Fock states, where ϵ_a^{HF} is the Hartree–Fock energy, f_a is the Fermi occupation factor and κ the dielectric constant of the surrounding medium. In terms of this basis set we will use the corresponding time-dependent HF (HF-RPA) to calculate the charge-density and spin-density correlation functions, which describe the self-consistent linear response of the electron gas to an external perturbation. In this letter, we restrict ourselves to the nonmagnetic ground state.

For inelastic light scattering not close to the band gap resonance, the Raman intensities in polarized and depolarized scattering geometries are proportional to the imaginary parts of the charge–charge correlation function and spin–spin correlation function [9], respectively. If we define $\hat{\rho}(\mathbf{q}, t)$ as the Fourier transform of the charge-density operator and $\hat{\sigma}(\mathbf{q}, t)$ as the Fourier transform of the spin-density operator along the spin quantization axis, then these correlation functions are $\chi^\nu(\mathbf{q}, \omega) = -\frac{i}{\hbar} \int_0^\infty dt e^{i\omega t} \langle | [\hat{\nu}(\mathbf{q}, t), \hat{\nu}(-\mathbf{q}, 0)] | \rangle$ with $\nu = \sigma, \rho$, where $\langle | \dots | \rangle$ denotes a thermodynamic average. In HF-RPA, they can be expressed as $\chi^\nu(\mathbf{q}, \omega) = \sum_{cd} K_{cd}^\nu(\mathbf{q}, \omega) \langle c | \exp -i\mathbf{q} \cdot \mathbf{r} | d \rangle$ in terms of the ν -density-induced matrix K^ν . The charge-density-induced matrix satisfies

$$K_{ab}^\rho(\mathbf{q}, \omega) = \frac{f_b - f_a}{\hbar\omega + i0^+ - (\epsilon_a^{HF} - \epsilon_b^{HF})} \left[2 \langle a | e^{-i\mathbf{q} \cdot \mathbf{r}} | b \rangle^* - \sum_{cd} (2V_{cb;ad} - V_{bc;ad}) K_{cd}^\rho(\mathbf{q}, \omega) \right] \quad (2)$$

where $V_{ab;cd} = \int d\mathbf{r} \int d\mathbf{r}' \Psi_a^*(\mathbf{r}) \Psi_d(\mathbf{r}) \Psi_b^*(\mathbf{r}') \Psi_c(\mathbf{r}') / |\mathbf{r} - \mathbf{r}'|$ is the Coulomb matrix element in the basis of the HF single-particle states. When $\nu = \sigma$ there is no direct Coulomb interaction (Hartree term) between the excited spins. If the exchange term (Fock term)

is neglected, the spin-density excitation spectra are simply given by the quasi-particle Hartree–Fock energies. In HF-RPA the spin-density excitations are shifted from the quasi-particle Hartree–Fock energies due to the exchange terms. As a result collective spin-density excitation may appear in the spectra. This shift is a measure of the effective strength of the exchange term in the system.

We will use the above HF-RPA analysis to investigate collective excitations in a multi-subband system. This has to be done numerically and the first step is to derive the quasi-particle basis set $\{\psi_a(\mathbf{r})\}$ by solving (1) self-consistently via iteration. The functional basis must be sufficiently large in order to ensure the required accuracy for the quasi-particle energy spectra and the spatial electron density of the ground state. When using this self-consistent quasi-particle basis set to calculate collective excitations the required accuracy for the peak position of an excitation energy is the experimental linewidth $\simeq 0.1$ meV.

The intrinsic materials parameters of a GaAs quantum wire required in our calculation are $m^* = 0.067m_0$ and $\kappa = 12.4$, where m_0 is the electron mass. The extrinsic sample parameters are the total electron density n , the transverse potential $V_c(y)$ and the length of the quantum wire L_x . Our calculations are based on a sample with $n = 10.4 \times 10^5 \text{ cm}^{-1}$, which has been investigated experimentally in [3]. The transverse potential $V_c(y)$ is determined by the experimental conditions. Since the experimental sample does not have a parabolic potential, as can be seen from the intersubband CDE, we will adjust $\hbar\omega_0$ to fit the subband electron occupations. When we set $\hbar\omega_0 = 7.9$ meV ($l_0 = 120 \text{ \AA}$), the derived self-consistent Hartree–Fock subband spacing between the two lowest subbands is 5.4 meV at the zone centre and 5.6 meV at the Fermi level. The electron densities in the two occupied subbands are $n_0 = 6.4 \times 10^5 \text{ cm}^{-1}$ for the lowest subband (labelled by $i = 0$) and $n_1 = 4.0 \times 10^5 \text{ cm}^{-1}$ for the second lowest subband (labelled by $i = 1$). The physical properties of the quantum wire are insensitive to its length, provided that the wire is sufficiently long. Therefore we set $L_x = 1.0 \text{ \mu m}$. The experiment [3] was done at 1.7 K, which is the temperature used in our calculation.

Let k_i and v_i be the Fermi wavevector and the Fermi velocity of the i th subband, respectively. In the limit of long wavelength $q \rightarrow 0$, the transverse excitation is forbidden (or allowed) if the excitation energy is low (or high), and so the corresponding physical processes are dominated by intrasubband (or intersubband) transitions. When q increases to k_0-k_1 , the low-energy intersubband transitions are activated. However, collective excitations with large energy and/or large q are strongly damped. In order to illustrate the main features of long-wavelength excitations, let us consider a very simple case, neglecting the electron self-energies and the vertex correction. In this case we obtain analytical results for both the SDE and CDE energies. The SDE dispersion is linear in q , with sound velocities v_0 and v_1 for intrasubband excitations in the two lowest subbands. With two subbands occupied, the CDE dispersion has two branches. The in-phase mode is

$$\omega_\rho^+(q) = |q| \sqrt{2(v_0 + v_1)V(q)/\hbar\pi} \quad (3)$$

where $V(q)$ is the Fourier transform of the Coulomb potential $(e^2/\kappa)[(x-x')^2 + (y-y')^2]^{-1/2}$ and the out-of-phase mode is

$$\omega_\rho^-(q) = |q| \sqrt{v_0 v_1}. \quad (4)$$

Such two-band SDE and CDE dispersions are exactly the same results as Schulz [10] obtained for a two-subband Tomonaga–Luttinger model (TLM) [11].

When we turn on the intrasubband and intersubband exchange interaction, as well as the screening, the SDE and CDE energies will be modified from the above expressions and have to be derived numerically. In the polarized spectrum, the higher-energy region is

dominated by strong intersubband CDE. At $q = 0$ the calculated CDE spectrum consists of a single peak which is characteristic of transverse parabolic confinement potentials [12]. In the region of finite q the intersubband HF SPE energies show up at 5.5 meV. In the spin-flip depolarized Raman spectrum, we obtained the red shift of intersubband SDE with respect to HF SPE. The SDE has the dominant weight of the spectrum and appears at a resonance energy of 2.1 meV which is shifted from the HF SPE, indicating the importance of vertex correction. These overall features of our numerical results have been observed experimentally [2, 3].

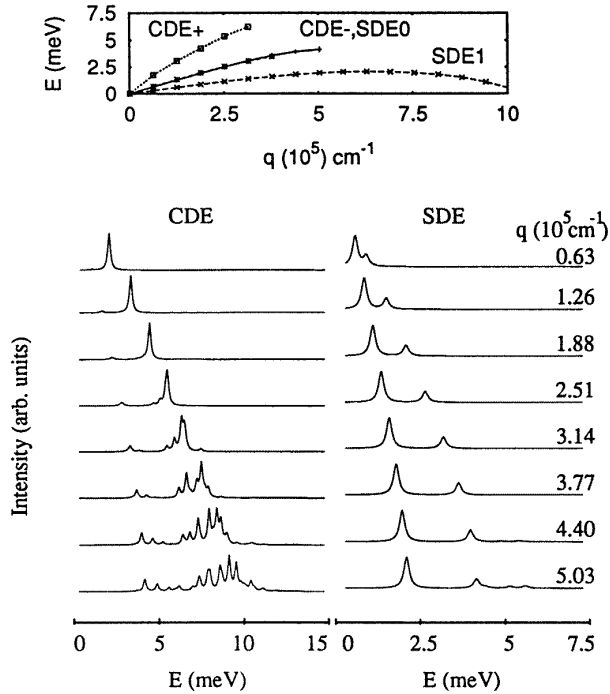


Figure 1. Intensity of intrasubband SDE and CDE as a function of the frequency shift for different wavevectors q . The upper part shows the dispersion of intrasubband CDE and intrasubband SDE. The quantum wire is specified in the text.

In figure 1 we show the calculated intrasubband SDE and CDE in the region of energy and frequency for which accurate experimental data are available. The mode with strong intensity is labelled SDE0 and the next mode with weaker intensity is labelled SDE1. The inset gives their dispersions, which are linear for small q , with the corresponding sound velocities $v_{\sigma,0} = 0.9v_0$ and $v_{\sigma,1} = 0.7v_1$. These sound velocities are smaller than the respective Fermi velocities because of the exchange screening of SDE induced by the intersubband virtual transitions, and the renormalization due to the intra- and intersubband exchange interaction. The experiments in [2] and [3] seem to have detected only $v_{\sigma,0}$, which corresponds to the high-energy SDE near the Fermi wavevector k_0 of the lowest subband. It is probably the low electron density in the second lowest subband that causes the velocity $v_{\sigma,1}$ of the SDE around k_1 to be too small to be observed experimentally. The spin velocity $v_{\sigma,0}$ agrees quantitatively with the experiment [3]. For sufficiently large q , because of the finite length of our quantum wire, the Landau damping shows up in figure 1 in the form

of enhanced intensities of satellite single-particle peaks around the SDE, instead of a broad band if the quantum wire is infinitely long. The mode SDE1 is not damped since it does not enter the region of SPEs.

The dispersions of the CDE and SDE are also plotted in the inset in figure 1. In the long-wavelength limit, the in-phase CDE+ can be well fitted with $q[-\ln(q)]^{-1/2}$ according to (3), as expected for a 1D electron gas [10, 13]. The out-of-phase CDE- mode, corresponding to (4) with an expected linear dispersion [10], appears in our calculation as a weak band with a sound velocity $1.2(v_0v_1)^{1/2}$. This happens to be the same as the sound velocity of the SDE0, an accidental result for this specific sample. The CDE- mode has a much lower intensity than the CDE+ mode. Checking against experiment [2], we believe the the lower energy band observed in the low-frequency polarized Raman spectrum is our calculated CDE- mode. The decay of the plasmon (CDE+) and the CDE- at higher q due to the Landau damping is stronger than the decay of SDE0 and SDE1, as shown in figure 1 .

After the above complete study of a realistic quantum wire perhaps it is worthwhile to mention some surprising findings for the special case in which only the lowest subband occupied at zero temperature, namely the pure 1D system including spin degrees of freedom. In this case we can drop the band index. For SDE, the eigenvalue equation has the form

$$K_k^\sigma(q, \omega) = -\frac{f_{k-q/2} - f_{k+q/2}}{\hbar\omega - (\epsilon_{k+q/2}^{HF} - \epsilon_{k-q/2}^{HF})} \frac{1}{2\pi} \int dk' V(k-k') K_{k'}^\sigma(q, \omega) \quad (5)$$

where $V(k) = (2e^2/\kappa)K_0(ql_0)$ for the quasi-1D Coulomb potential $(e^2/\kappa)[(x-x')^2 + l_0^2]^{-1/2}$ which has a logarithmic singularity $(-2e^2/\kappa) \ln ql_0$ as $q \rightarrow 0$. Since the Hartree self-energy is cancelled by the potential energy due to the positive background charges, the difference in exchange self-energy at the Fermi energy, $\Delta_x(q) = \Sigma_x(k_0 + q/2) - \Sigma_x(k_0 - q/2)$ is $\Delta_x(q) = \frac{1}{2\pi} \int_{-q/2}^{q/2} dk' [V(k') - V(k' - 2k_0)]$.

We define $y(k)$ by $K_k^\sigma \equiv (f_{k-q/2} - f_{k+q/2})y(k)$, and at $k = k_0$ rewrite (5) as

$$\int_{-q/2}^{q/2} dk' [-V(k')y(k_0 + k') + V(k' - 2k_0)y(-k_0 + k')] = 2\pi [\hbar\omega - \hbar qv_0 - \Delta_x(q)] y(k_0). \quad (6)$$

In the limit of long wavelength, by substituting $y(k_0 + k') \simeq y(k_0)$ and $y(-k_0 + k') \simeq y(-k_0)$ into the above equation, we see that the contributions of Coulomb potential in the exchange energy and the vertex corrections, both behave as $q \ln(q)$, exactly cancelling each other. Hence, the $q \ln(q)$ behaviour of low-energy single-particle excitation due to the exchange self-energy is removed from the SDE and the plasmon energies, and so only the exchange terms at momentum $2k_0$ are important. An equation similar to (6) for y_k at $k = -k_0$ can also be derived. In the long-wavelength limit we find the SDE energy

$$\omega_\sigma(q) = |q|v_0\sqrt{1 - 2g_0} \quad (7)$$

where $g_0 = V(2k_0)/2\hbar\pi v_0$. The sound velocity is reduced with respect to the bare Fermi velocity. We have also solved for the CDE and found the plasmon dispersion

$$\omega_\rho(q) = |q|v_0\sqrt{2V(g)/\hbar\pi + 1 - 2g_0}. \quad (8)$$

For a long-range Coulomb potential $V(q) \sim \ln q$, the plasmon energy is not affected by the exchange interaction within the HF-RPA. These results, (7) and (8), derived with full Coulomb interaction, differ from those obtained by Schulz [10] for the TLM including a nonsingular backscattering matrix element at $2k_0$, which mixes the right- and the left-travelling modes. Nevertheless, if we replace the Hartree-Fock energy in (5) by the bare

single-particle energy and omit the singular part around $V(q = 0)$ in the vertex correction, then our results exactly reduce to Schulz's results for the SDE and the plasmon energies. Whether this finding, as well as (3) and (4), is simply a coincidence remains to be clarified.

To close this letter, we should mention that according to our analysis, the frequency of the lowest-energy SDE decreases as q increases towards k_1 , and then vanishes at a value of q close to $2k_1$. This behaviour suggests a low-temperature intrinsic instability of the electron gas against the formation of spin-density waves (SDW), namely the Peierls instability. When this instability emerges from our mean-field analysis, we must take into account the SDW long-range order in the ground state. On the other hand, the results of the TLM with backscattering predict the absence of SDW long-range order but instead the appearance of a slowly decaying Wigner crystal at $4k_F$ [10]. We guess that the TLM with backscattering describes the real ground state better than HF-RPA. Hence, we believe that our analysis based on a ground state without SDW long-range order is a better approximation than that including SDW in the ground state.

AB would like to thank A Sudbø and L J Sham for stimulating discussions. This research was supported in part by a NorFa Grant.

References

- [1] Egeler T *et al* 1990 *Phys. Rev. Lett.* **65** 1804
- [2] Goñi A R *et al* 1991 *Phys. Rev. Lett.* **67** 3298
- [3] Schmeller A *et al* 1994 *Phys. Rev. B* **49** 14 778
- [4] Ando T 1982 *J. Phys. Soc. Japan* **51** 3893
- [5] Katayama S and Ando T 1984 *J. Phys. Soc. Japan* **54** 1615
- [6] Tselis A C and Quinn J J 1984 *Phys. Rev. B* **29** 3318
- [7] Eliasson G, Hawrylak P and Quinn J J 1987 *Phys. Rev. B* **35** 5569
- [8] Baym G and Kadanoff L P 1961 *Phys. Rev.* **124** 287
- [9] Hamilton D C and McWhorter A L 1969 *Light Scattering Spectra of Solids* ed G B Wright (New York: Springer)
- [10] Schulz H J 1993 *Phys. Rev. Lett.* **71** 1864
- [11] Haldane F D M 1981 *J. Phys. C: Solid State Physics* **14** 2585
- [12] Kohn W 1961 *Phys. Rev.* **123** 1242
- [13] Li Q and Sarma S D 1989 *Phys. Rev. B* **40** 5860